We thank the two Referees for careful reading of the manuscript and positive evaluation of our work. Both reviewers made two identical suggestions on the improvement of the manuscript: (i) A request for some quantitative support of the counteracting effect on long-term lake temperature evolution of the increasing air temperature and decreasing solar radiation amount; (ii) a recommendation to provide some basic details on the model used in the study. We reply first to these two remarks and address the other minor remarks afterwards.

Our responses are marked in **bold face**, the outtakes from the revised manuscript are in *italic*.

General reply 1. (Referee I, remark 2. Referee II, remark 1) Justification of the canceling effect of the radiation decrease on the water temperature trend.

We agree that a more detailed quantitative analysis of the long-term effects of the atmospheric trends would provide a stronger support to the suggested cause of the negligible lake warming over Tibet. We performed a set of model sensitivity experiments on this subject and described the outcomes in the Discussion part of the manuscript as follows:

"To quantify the counteracting effects of the increasing air temperature and the decreasing short-wave radiation we performed model runs using artificial short-wave radiation input constructed from ERA values (which had a significant negative trend) with the summer radiation trend removed. The trend was removed based on daily averaged values, and the diurnal cycle of solar radiation was subsequently restored to the detrended values based on daytime duration and the daily maxima of solar radiation. Additionally, a 'control' model run was performed with the radiation input reconstructed from daily averages using the same procedure, but without trend removal. The model results based on the modified 'control' radiation input did not differ significantly from those based on the original ERA input (not shown). In turn, the model driven by the detrended radiation input produced a positive trend in the mean summer surface temperature of 0.26 °C decade^{-1} and the maximum summer surface temperature of 0.34 °C decade^{-1}. The trend in surface water temperatures was significant at > 99% level of confidence (p = 0.003), whereas the original ERA input produced no significant long-term increase of surface temperatures (0.15 °C decade^{-1} at < 93% level of confidence, see Table 4). Hence, the short-wave radiation decrease did indeed cancel the effect of the air temperature increase on lake temperatures in ERA-driven scenarios. The hypothetical surface temperature trend 0.26 °C decade^{-1} is still lower than the summer air temperature increase of 0.50 °C decade^{-1}, and is accompanied by significant changes in the summer stratification: a later breakdown of the stratification due to autumn cooling (1.8 days decade^{-1}, p = 0.034) and a shallower surface mixed layer depth (0.14 m decade^{-1}, p = 0.006). Several previous studies devoted to alpine or tropical lakes also reported lake temperature trends lower than the regional atmosphere warming (Livingstone 2003; Vollmer et al. 2005; Coats et al. 2006), *while lowland temperate lakes are often found to be in a thermal equilibrium with the atmosphere* (Arhonditsis et al. 2004; Danis et al. 2004; Kirillin 2010)."

2. In reply to the Referees' request (Referee I, Remark 3 and Referee II. Remark 2) we included a description of the model concept and additional references to the Methods":

For completeness, we provide here a short description of the model concept, following Kirillin (2010). *For further details the reader is referred to the model manual* (Mironov 2008). *FLake is a one-dimensional model calculating the evolution of the horizontally averaged temperature in lakes. The basic principle underlying the model consists in splitting the water column into horizontal layers of variable depth, using physically-motivated assumptions about their properties, and subsequently integrating the governing equations over these layers. In this sense, FLake belongs to the family of*

bulk-models, of which the mixed layer models of the oceanic surface boundary layer (Niiler and Kraus 1979) are the most famous examples. In contrast to the traditional mixed-layer models, FLake additionally involves the "thermocline self-similarity" hypothesis to describe the lower stratified layer. The idea consists in adopting the thermocline thickness, $\Delta h(t)$, and the temperature jump across the thermocline, $\Delta T(t)$, as universal scales for the temperature profile, $T(t, z,)$ (Fig. 2). Using these scales, the dimensionless temperature, ϑ, and the dimensionless vertical coordinate, ζ, can be introduced as

$$\vartheta = \frac{T(t,z) - T_S(t)}{\Delta T(t)}, \ \zeta = \frac{z - h(t)}{\Delta h(t)} \ , \tag{1}$$

where T_S is the temperature in the surface mixed layer and h is the mixed layer depth. The self-similarity of the temperature profile implies universality of the function $\vartheta(\zeta)$, or, in other words, a universal shape of the temperature profile within the stratified layer of all lakes. Several analytical expressions for $\vartheta(\zeta)$ have been proposed by various authors that all represent a similar thermocline shape supported by numerous observations (see the comprehensive review by Kirillin 2002). Assuming a two-layer lake temperature structure with a homogeneous upper layer and a self-similar stratified layer beneath, the vertical temperature profile across the entire water column can be described as (Fig. 2),

$$T(t,z) = \begin{cases} T_S(t) & at & 0 \leq z \leq h(t) \\ T_S(t) - \vartheta(\zeta)\Delta T(t) & at & h(t) \leq z \leq h(t) + \Delta h(t) \end{cases} . \tag{2}$$

The temperature profile represented by Eq. (2) does not depend explicitly on the vertical coordinate, which allows the heat transport equation to be integrated across the layers $0 < z < h$ and $h < z < (h+\Delta h)$, turning the partial differential equation for $T(t,z)$ into a set of two ordinary differential equations (ODEs). The same self-similarity concept is used to describe the temperature structure of the thermally active upper layer of the bottom sediments (Golosov and Kirillin 2010) and of the ice cover (Mironov et al. 2012), so that the model, strictly speaking, is four-layered, with a unique self-similarity function $\vartheta(\zeta)$ for every layer: ice (if it exists), the mixed layer, the stratified layer, and the thermally-active sediment. Integration of the turbulent kinetic energy (TKE) equation across the upper mixed layer (Niiler and Kraus 1979) yields an additional ODE for the evolution of the mixed layer depth, h(t). The derivation procedure and the exact ODE expressions are given by Mironov (2008). The surface boundary conditions enter the reformulated problem as the time-dependent functions for the surface heat and momentum fluxes; the latter is used in the TKE equation for estimating the impact of the wind-generated mixing on the mixed layer h(t) evolution. The short-wave solar radiation is not included into the boundary condition for the surface heat flux, but is treated as a separate heat source absorbed internally within the upper water column by the one-band exponential law for radiation decay. A separate model block calculates the surface heat and momentum fluxes from the standard meteorological variables and the water surface temperature at the previous time step (Mironov 2008).

<u>Referee 1</u>.

1. The authors tend to extend their findings and conclusions onto all lakes of the Tibetan highlands, which are "thousands" distributed over a broad area, while factually they only investigated two

individual lakes, situated close to each other. Therefore, they should either confine their conclusions to the specific lakes Ngoring and Gyaring (perhaps, making it explicit even in the title of the article), or otherwise try to justify that these two lakes are somehow representative of the whole generality of Tibetan lakes. Is it possible to compile from the literature some kind of statistics on the principal characteristics of all Tibetan lakes (e.g., size, depth, salinity, turbidity, etc) from where it would follow that Ngoring and Gyaring are indeed "typical" examples?

Reply: we did not claim the two investigated lake were 'typical' for the very versatile lake system of Tibet. They are the two largest freshwater lakes of the system. However, our methods of analysis, including modeling, allow to extend the majority of our findings on the freshwater lakes on the Plateau. We believe, no changes are necessary in the title. We clarified our point in the following text added to the discussion:

Our model experiments are well supported by the observational data from the largest freshwater lake of the Tibetan Plateau. They compare the dynamics of lakes with different depths and water transparencies under the same atmospheric forcing, characteristic for high-altitude conditions. The presented results provide the first detailed insight into the specific mechanisms of internal lake mixing and lake-atmosphere coupling, specific to the Tibetan lakes and extendable to other high-altitude hydrological systems. It should be noted that freshwater lakes comprise only about 10% of the Tibetan lake system (Jiang and Huang 2004), while ~75% of lakes have brackish or saline water (the salt content of the rest of lakes is unknown). The salt stratification can significantly contribute to the seasonal mixing regime as well as to the lake response to long-term changes in the atmospheric input. Effects of salinity, as well as lake physics during the ice-covered period, as discussed above, are the two major facets of lake dynamics for further clarification with regard to specific features of the Tibetan lake system.

2. The core result of the present study, as the authors put it, is the statement that on the climatic scale, "the effects of the air temperature increase on the lake heat budget were counteracted by the reduced radiative heating". While this concept is qualitatively clear and sounds very plausible, cannot it be made more quantitative? That is, can we estimate the changes which the air temperature trend of 0.5-0.7oK decade-1 evident in the reanalysis will produce in the heat flux through the lake surface and see whether the latter is sufficient to offset the decrease of solar irradiance at 3.8 W m-2 decade-1? If yes, this would make the author's hypothesis about the mutual compensation of the two trends in heat budget components much more grounded.

See General Reply 1.

Specific comments

3. In my opinion, the description of the FLake model (section 2.3) should be detalized and made more concrete. It is not immediately clear to those unfamiliar with the model what does "self-similar representation of the temperature profile" mean (do I understand right that the shape of the profiles is prescribed and only the coefficients are fitted?) and what kind of prognostic entrainment equation was used. Of course, these details can be found in the references provided by the authors, but the reader should be able to get sufficient insight into the model without having to browse through the literature.

See General Reply 2.

4. Figure 3 is barely legible at this scale. For example, the thin grey line is only distinguishable where the NCEP/NCAR-forced outcome exceeds the ERA-force one. I suggest simply deleting this figure, as it adds little, if anything, to the information already presented in the tables.

Reply: while we partially agree on the comment, we decided to keep the figure as demonstrating the available satellite data and providing a visual demonstration of the impossibility of trend simation based on the remote sensing only (see our reply to the comment on P8L28 of Reviewer II).

5. Page 3, lines 31-32: "The mineralization of the lake water is low with a conductivity of ~0.4 mS/cm-1" – can this be expressed in mg/l of salt content?

Reply: Since exact information on salt content is absent for both lakes, and the conductivity values are superfluous for the subsequent analysis we replaced the sentence with:

Also, both lakes are fresh, with salt content < 1 g l^{-1} (Kar 2014), so that effects of salt on density stratification can be neglected in modeling.

6. Same lines and page 4, first paragraph: Mineralization is specified only for Ngoring, while nothing is said about mineralization of Gyaring. Reciprocally, the Secchi depth is only specified for Gyaring, with no mention of that in Ngoring. This is confusing. Whenever possible, comparative characteristics should be given for both lakes.

Reply: the Secchi depth has been given for both lakes. The text has been refined to make it unambiguous (Section 2.1 Study sites).

7. Page 7, line 4: Looks like Fig. 4 is referred to before Fig. 3. Consider revising the numbering of figures.

Reply: figures are re-ordered and the numbering is made consistent.

<u>Referee 2</u>.

1- Though sound, the conclusion about the counteracting effects of increasing air temperature and decreasing radiation is a bit hypothetical in the present form. It would strengthen the conclusion if the authors quantified the expected effect of the decreas-ing radiation on the lake temperature, and the expected effect of the warming air temperature on the heat budget component and to compare them.

See General Reply 1.

2- a brief description of the Flake model would be beneficial to a smooth reading, since some detailed aspects of the physics included or not in the model are discussed in the model performance section. Also in the discussion of the model performance, the judgment words (appreciably better, etc. . .) could be backed up by basic statistics.

See General Reply 2.

Minor comments:

P1L21 and elsewhere: dampened should be damped

We replaced dampened with damped.

P1L22: I would recommend specifying "the modeled mean lake temperatures did not change".

Reply: added.

P4L12: what is the time resolution of the bulk temperature? "All sensors . . .recorded the same temperatures": are you referring to diurnal averages?

Reply: Even at sub-diurnal time scales, the upper 0.6 m of the water column remained well-mixed within the 0.1°C accuracy of the sensors.

P5L11: is there a mismatch in the figure? There seems to be more open water points than what the figure shows.

Reply: one of the earlier versions of the figure missed one open water open water point in Gyaring. There are 5 and 8 open points for Gyaring and Ngoring respectively.

P8L28: it could be nice to add a small note on the trend in the satellite measurements as comparison (since there are several decades available).

Reply: we considered this option during the analysis but had to abandon it. An explanation is added to the revised manuscript as:

The satellite data on lake surface temperatures, despite the coverage of several decades, were found inappropriate for reliable trend estimation due to numerous data gaps of several months, exceeding the half-period of the seasonal variations (Fig. 3)

P9L30: please provide some details about these bulk algorithms.

Reply: We extended the sentence as following:

Taking into account strong constraints on the computational costs of the lake parameterization schemes, a remarkable improvement in regional climate models can be achieved by extending the lake modules to include one of the bulk algorithms developed earlier for convective mixing based on integration across the mixed layer of the equation for mixing energy production with solar radiation as a volumetric energy source (Mironov et al. 2002; Oveisy and Boegman 2014).

P11L26: Is the mixed layer thickness not an output of the model? If so, can the evolution in time of the modelled mixed layer thickness confirm the argument?

Reply: the argument is based on the modeling results on the mixed layer trends (last paragraph of Results).

Seasonal thermal regime and climatic trends in lakes of <u>the</u> Tibetan Highlands

Georgiy Kirillin[1], Lijuan Wen[2], Tom Shatwell[1]

5   [1]Department of Ecohydrology, Leibniz-Institute of Freshwater Ecology and Inland Fisheries (IGB). Berlin, 12587 Germany

[2]Key Laboratory of Land Surface Process and Climate Change in Cold and Arid regions, Northwest Institute of Eco-Environment and Resources, Chinese Academy of Sciences, Lanzhou , 73000 China

Correspondence to: Georgiy Kirillin (kirillin@igb-berlin.de)

10   **Abstract.** The hydrology of the lake-rich Tibetan Plateau is important for the global climate yet little is known about the thermal regime of Tibetan lakes due to scant data. We (i) investigated the characteristic seasonal temperature patterns and recent trends in thermal and stratification regime of lakes on the Tibetan Plateau and (ii) tested the performance of the one-dimensional lake parameterization scheme FLake for the Tibetan lake system. For this purpose we combined three years of in situ lake temperature measurements, several decades of satellite observations and the global reanalysis data. We chose the two

15   largest freshwater Tibetan lakes—Ngoring and Gyaring— as study sites. The lake model FLake faithfully reproduced the specific features of the high-altitude lakes and was subsequently applied to reconstruct the vertically resolved heat transport in both lakes during the last four decades. The model suggested Ngoring and Gyaring were ice-covered for about 6 months and stratified in summer for about 4 months per year with a short spring overturn and longer autumn overturn. In summer the surface mixed boundary layer extended to 6 – 8 m depth and was about 20% shallower in the more turbid Gyaring. The thermal

20   regime of transparent Ngoring responded more strongly to atmospheric forcing than Gyaring, where the higher turbidity ~~dampen~~<u>damp</u>ed the response. According to reanalysis data, air temperatures and humidity increased, whereas solar radiation decreased since the 1970s. Surprisingly, <u>the modeled</u> mean lake temperatures did not change, nor did the phenology of ice cover or stratification. Lake surface temperatures in summer increased only marginally. The reason is that the increase in air temperature was offset by the decrease in radiation, probably due to increasing humidity. This study demonstrates that air

25   temperature trends are not directly coupled to lake temperatures and underscores the importance of short-wave radiation for the thermal regime of high-altitude lakes.

1 Introduction

The hydrological regime of the Tibetan highlands is extremely complex and highly sensitive to climate changes (Gu et al. 2005; Ma et al. 2012; Yang et al. 2014). The Plateau of Tibet plays a crucial role in the global water cycle because it directly

30   affects the monsoon system and is the origin of major Asian rivers (Su et al. 2015) including the Yellow, Yangtze, Mekong,

1

Salween, Brahmaputra (Yarlung Tsangpo), and Indus Rivers (Fig. 1). The Plateau contains thousands of lakes, whose hydrological regime is closely connected to glaciers, permafrost, as well as in- and effluents (Zheng 2011; Zhang et al. 2013). The particular climatic environment of the Tibetan Plateau, with low air pressure and intense solar radiation, creates a unique land-atmosphere interaction (Ma et al. 2009), where the lake system is a crucial component of the regional heat and mass balance (Liu et al. 2009; Gerken et al. 2013; Li et al. 2015; Wen et al. 2015; Dai et al. 2016). Therefore, changes in the regional water budget of the Tibetan Plateau driven by global warming are of key importance for climatic changes on continental scales. Recent evidence indicates that the number of lakes on the Tibetan Plateau is increasing, highlighting global warming effects and local anthropogenic activity, such as infrastructure construction on permafrost (Cheng and Wu 2007; Liu et al. 2009; Yang et al. 2010). Hence, to estimate how lakes may affect the regional climate, it is necessary to quantify the seasonal thermal dynamics of lakes and ponds, with particular reference to the vertical thermal stratification, the ice regime, and the lake interactions with the lower atmosphere.

Due to the importance of lakes for understanding the global-scale changes on the Tibetan Plateau, several studies have been performed in recent years on lake dynamics and lake-atmosphere interactions. The amount of evaporation and heat flux, and their change, were revealed in lakes in the Tibetan Plateau during the pre- and post-monsoon periods (Haginoya et al. 2009; Xu et al. 2009). Biermann et al. (2014) measured the turbulent fluxes over wet grassland and a shallow lake with the eddy covariance method at the shoreline in the Lake Nam Co basin. Li et al. (2015) recently studied the characteristics of the energy flux and the radiation balance over Ngoring Lake. With the development of lake schemes and atmospheric models that include the lake surface (Sun et al. 2007), other studies have investigated the effects of the Tibetan Plateau lakes on local climate (Li et al. 2009; Wen et al. 2015; Yang et al. 2015). Nevertheless, compared to other lake-rich regions of the world, like Fennoscandia, Northern Canada, or the East-Siberian Tundra, the lakes of the Tibetan Plateau are poorly studied, despite their extraordinary thermal regimes due to strong seasonal and synoptic variations.

A major problem in resolving the energy and moisture budget of high-altitude lakes is the lack of long-term observations. Observational data on the physics of Tibetan Plateau lakes are scarce and mostly confined to remote sensing data on lake surface characteristics, such as lake surface temperature (Lin et al. 2011; Zhang et al. 2014). Observations of air-lake fluxes using eddy covariance methods over Tibetan Plateau lakes are too fragmentary to estimate the seasonal variations (Biermann et al. 2014; Li et al. 2015). Furthermore, lack of knowledge of the heat transport within the lake water column, including seasonal formation of thermal stratification, and thermal dynamics under ice cover, have limited our understanding of lake-atmosphere interactions on climatic scales.

While first brief reports were recently presented (Wang et al. 2014; Wen et al. 2016) on the mixing conditions and vertical heat transport within the lake water bodies, there are no observational data covering the annual variability or long-term trends in thermal conditions and stratification in Tibetan lakes since no regular lake monitoring was performed in this area in the past. In this situation, modeling of decadal variability in lake dynamics can provide an insight into the ongoing changes on seasonal to climatic time scales, provided that model performance is tested against available observational data on shorter periods. On the other hand, validation of models for parameterizing lakes in weather prediction and climate studies is of significant value

2

per se, particularly because it is crucial to properly account for the heat budget of one of the largest lake systems worldwide to adequately model heat and mass transport on a planetary level.

In view of these challenges, the present study aimed to:

- Characterize the seasonal stratification regime and ice cover formation in lakes of the Tibetan Plateau using the two largest freshwater lakes of the region as examples.

- Test the ability of the lake model FLake (Mironov 2008; Kirillin et al. 2011) to simulate the main features of the lake thermodynamics in high-altitude conditions as a potential tool to parameterize the Tibetan lake system in regional climate modeling.

- Quantify the mean trends in the thermal and ice regime of Tibetan lakes during the last half-century and to estimate the climate-driven changes in the seasonal stratification pattern.

For this purpose we combine 3-year observations on the surface heat budget from Ngoring Lake (Wen et al. 2016) with the surface temperatures from the AVHRR SST product (Casey et al. 2010), the one-dimensional lake temperature and mixing model FLake and the long-term forcing from the ERA-Interim and NCEP/NCAR global atmospheric reanalyses (Kalnay et al. 1996; Dee et al. 2011). In situ and satellite data on the surface temperatures are primarily used to validate the model performance at short and long time scales, respectively. The model is forced by reanalysis data in two different configurations, corresponding to the two neighboring large freshwater lakes located in the north-eastern part of the Plateau—Ngoring and Gyaring. Both lakes undergo virtually the same atmospheric forcing, but differ in mean depth and water transparency. Therefore, a comparison of the model results allows not only quantifying the seasonal and climatic characteristics of the mixing regime, but also estimating the response of the lake thermal structure to variations in the subsurface radiation regime and total depth of the water column.

2 Methods

2.1 Study sites

Ngoring (Big Blue Lake) and Gyaring (Big Gray Lake), sometimes referred as the 'twin lakes', are two large freshwater lakes in the source region of the Yellow River (Huang He) on the eastern Tibetan Plateau (Fig. 1). The lakes are located at 34.5-35.5°N and 97-98°E, less than 50 km from each other, at an altitude of ~4300 m a. s. l., which counts them among the world's highest freshwater lakes. The Yellow River flows through both Gyaring and Ngoring. The lakes are surrounded by hills covered with alpine meadows. Cold semi-arid continental climate prevails in the lake basin, and the long-term (1953–2012) monthly mean air temperature varies from 7.7 °C in July to -16.2 °C in January, with an annual mean of -3.7 °C (Li et al., 2015); the average annual precipitation is 321.4 mm (Data from China's National Climate Center). The lakes are ice-covered from early December to mid-April.

Ngoring Lake has a surface area of 610 km^2. The mean and maximum depths are 17 and 32 m, respectively. ~~The mineralization in the lake water is low with a conductivity of ~ 0.4 mS cm^{-1}.~~ The lake is oligotrophic, fish in the lake are rare, and aquatic

3

plants grow only in the riparian areas. The reported lake water transparency (Secchi depth) does not exceed 3m (Kar 2014). Gyaring Lake has a similar surface area (526 km^2) but is shallower than Ngoring Lake with an average depth of 8.9 m and maximum depth of 13.1 m. Lake water is more turbid than in Ngoring, with Secchi depth (transparency) of only 1 m (Kar 2014). Due to the close geographical location and similar surface areas, both lakes are subject to virtually the same atmospheric
5   forcing, but differ in their depths and water transparency – two major factors determining radiative heat transport within the water column and formation of thermal stratification. Also, both lakes are fresh, with salt content < 1 g l^{-1} (Kar 2014), so that effects of salt on density stratification can be neglected in modeling.

2.2 Lake temperature data

The lake-atmosphere heat exchange and characteristics of the air-lake boundary layer were systematically observed over
10 Ngoring Lake during the summer open water seasons of 2011-2013 (Li et al. 2015; Wen et al. 2015; Li et al. 2016; Wen et al. 2016). The bulk surface temperatures obtained in these observations comprise the primary dataset for verifying the lake model in this study. The bulk temperatures of the lake surface water were recorded by 109L probes (Campbell Scientific, Inc.) at water depths of 0.05, 0.20, 0.40 and 0.60 m during the observation period. All sensors in the 0.6 m thick surface layer recorded essentially the same temperatures within the probes' accuracy, so the 4 time series were vertically averaged for the subsequent
15 analysis. The incoming and outgoing shortwave and longwave radiation were measured with a net radiometer (CNR-1/CNR-4, Kipp and Zonen) 1.5 m above the lake.

2.3 Modeling

Modeling was performed with the lake temperature and mixing model FLake (Mironov 2008; Kirillin et al. 2011)—a highly parameterized bulk model of the lake thermal regime specifically designed to parameterize inland waters in regional climate
20 models and numerical weather prediction. The integrated approach implemented in FLake allowsed the combination of combining high computational efficiency with realistic representation of the major physics behind turbulent and diffusive heat exchange in the stratified water column. As a result, FLake is widely used for lake representation in land schemes of regional climate models, being implemented, among others, into the surface schemes of the Weather Research and Forecasting model (WRF, Mallard et al. 2014), HTESSEL (ECMWF, Dutra et al. 2010), SURFEX (Meteo France, Salgado and Le Moigne 2010),
25 and JULES (UK Met Office, Rooney and Jones 2010). Thanks to its robustness and computational efficiency, FLake has become a standard choice in climate studies involving the feedbacks between inland waters and the atmosphere, and is used operationally in the NWP models of the German Weather Service (DWD), the European Centre for Medium-Range Weather Forecasts (ECMWF), the UK Met Office, the Swedish Meteorological and Hydrological Institute (SMHI), the Finnish Meteorological Institute (FMI) and others.

30

For completeness, we provide here a short description of the model concept, following Kirillin (2010). For further details the reader is referred to the model manual (Mironov 2008). FLake is a one-dimensional model calculating the evolution of the

4

horizontally averaged temperature in lakes. The basic principle underlying the model consists in splitting the water column into horizontal layers of variable depth, using physically-motivated assumptions about their properties, and subsequently integrating the governing equations over these layers. In this sense, FLake belongs to the family of bulk-models, of which the mixed layer models of the oceanic surface boundary layer (Niiler and Kraus 1979) are the most famous examples. In contrast to the traditional mixed-layer models, FLake additionally involves the "thermocline self-similarity" hypothesis to describe the lower stratified layer. The idea consists in adopting the thermocline thickness, $\Delta h(t)$, and the temperature jump across the thermocline, $\Delta T(t)$, as universal scales for the temperature profile, $T(t, z,)$ (Fig. 2). Using these scales, the dimensionless temperature, ϑ, and the dimensionless vertical coordinate, ζ, can be introduced as

$$\vartheta = \frac{T(t,z) - T_S(t)}{\Delta T(t)}, \quad \zeta = \frac{z - h(t)}{\Delta h(t)}. \tag{1}$$

where T_S is the temperature in the surface mixed layer and h is the mixed layer depth. The self-similarity of the temperature profile implies universality of the function $\vartheta(\zeta)$, or, in other words, a *universal shape* of the temperature profile within the stratified layer of all lakes. Several analytical expressions for $\vartheta(\zeta)$ have been proposed by various authors that all represent a similar thermocline shape supported by numerous observations (see the comprehensive review by Kirillin 2002). Assuming a two-layer lake temperature structure with a homogeneous upper layer and a self-similar stratified layer beneath, the vertical temperature profile across the entire water column can be described as (Fig. 2),

$$T(t, z) = \begin{cases} T_S(t) & \text{at} & 0 \le z \le h(t) \\ T_S(t) - \vartheta(\zeta)\,\Delta T(t) & \text{at} & h(t) \le z \le h(t) + \Delta h(t) \end{cases}. \tag{2}$$

The temperature profile represented by Eq. (2) does not depend explicitly on the vertical coordinate, which allows the heat transport equation to be integrated across the layers $0 < z < h$ and $h < z < (h+\Delta h)$ turning the partial differential equation for $T(t,z)$ to a set of two ordinary differential equations (ODE's). The same self-similarity concept is used to describe the temperature structure of the thermally active upper layer of the bottom sediments (Golosov and Kirillin 2010) and of the ice cover (Mironov et al. 2012), so that the model, strictly speaking, is four-layered, with a unique self-similarity function $\vartheta(\zeta)$ for every layer: ice (if it exists), the mixed layer, the stratified layer, and the thermally-active sediment. Integration of the turbulent kinetic energy (TKE) equation across the upper mixed layer (Niiler and Kraus 1979) yields an additional ODE for the evolution of the mixed layer depth, $h(t)$. The derivation procedure and the exact ODE expressions are given by Mironov (2008). The surface boundary conditions enter the reformulated problem as the time-dependent functions for the surface heat and momentum fluxes; the latter is used in the TKE equation for estimating the impact of the wind-generated mixing on the mixed layer $h(t)$ evolution. The short-wave solar radiation is not included into the boundary condition for the surface heat flux, but is treated as a separated heat source absorbed internally within the upper water column by the one-band exponential law for radiation decay. A separate model block calculates the surface heat and momentum fluxes from the standard meteorological variables and the water surface temperature at the previous time step (Mironov 2008).

FLake is based on a two-layer parametric representation of the vertical temperature structure. The upper layer is treated as well-mixed and vertically homogeneous. The structure of the lower stably-stratified layer, the lake thermocline, is parameterized using a self-similar representation of the temperature profile. The same self-similarity concept is used to describe the temperature structure of the thermally active upper layer of the bottom sediments (Golosov and Kirillin 2010) and the ice cover (Mironov et al. 2012). The depth of the mixed layer is computed from the prognostic entrainment equation in convective conditions, and from the diagnostic equilibrium boundary-layer depth formulation in conditions of wind mixing against the stabilizing surface buoyancy flux.

The integrated approach implemented in FLake allowed combining high computational efficiency with realistic representation of the major physics behind turbulent and diffusive heat exchange in the stratified water column. As a result, FLake is widely used for lake representation in land schemes of regional climate models, being implemented, among others, into the surface schemes of the Weather Research and Forecasting model (WRF, Mallard et al. 2014), HTESSEL (ECMWF, Dutra et al. 2010), SURFEX (Meteo-France, Salgado and Le Moigne 2010), and JULES (UK Met Office, Rooney and Jones 2010). Thanks to its robustness and computational efficiency, FLake has become a standard choice in climate studies involving the feedbacks between inland waters and the atmosphere, and is used operationally in the NWP models of the German Weather Service (DWD), the European Centre for Medium-Range Weather Forecasts (ECMWF), the UK Met Office, the Swedish Meteorological and Hydrological Institute (SMHI), the Finnish Meteorological Institute (FMI) and others.

2.4 Lake temperatures from SST Pathfinder product

As an additional source of the lake surface temperature estimations, we used AVHRR Pathfinder Version 5.2 (PFV5.2) remote sensing data, obtained from the US National Oceanographic Data Center and GHRSST (http://pathfinder.nodc.noaa.gov). The PFV5.2 data are an updated version of the Pathfinder Version 5.0 and 5.1 collection described in Casey et al. (2010). Among the available lake surface temperature products, the AVHRR Pathfinder data have the longest time coverage (1982-2012) and a 4 km spatial resolution, distinguishing both Gyaring and Ngoring as water surfaces. The lake mask of the PFV5.2 includes 25 grid points for Gyaring, 5 of which are 'open water' points not adjoining the lake shoreline, and 31 points for Ngoring, 8 of which are 'open water' points. In the further analysis, only spatial averages of water temperatures from the open water points were used (Fig. 1) to reduce the potential influence of the surrounding land on the temperature readings.

2.5 Long-term model forcing from reanalysis data

In the absence of direct climatic observations for the study area, we adopted two widely used global reanalyses of atmospheric fields, the NCEP/NCAR Reanalysis 1 (previously NCEP/NCAR Reanalysis 40, Kalnay et al. 1996), and the ERA Interim Reanalysis produced by the European Centre for Medium-Range Weather Forecasts (ECMWF, Dee et al. 2011). Both datasets rely on different atmospheric models and data assimilation schemes. Accordingly, we first compared the surface layer

6

meteorology of the Tibetan Plateau from the two reanalysis datasets, and then we investigated how the surface meteorology affected the modeled lake physics. The parameters used to force the lake model were 6-hour surface layer characteristics: 2-m air temperature T_a [recalculated to °C], 2-m air humidity e_a [mb], incoming solar radiation I_R [W m^{-2}], 10-m wind speed U_{10} [m s^{-1}], and total cloud cover N [0-1]. The period 1975-2014 was applied for modeling forced by NCEP/NCAR, and a shorter

5   period of 1979-2014 was used for the ERA-driven modeling, since the ERA Interim data are available since 1979.

2.6 Model setup and validation

We avoided tuning the model-specific parameters and algorithms to the observed lake data, with the exception of the lake heat content at the initial stage of the open water season. The water temperature immediately after the ice breakup was set to 4°C independently of the modeled water temperatures during the preceding ice cover period. This amendment aimed to account

10   for heating of the water column by solar radiation during the ice covered period, which is not considered in the current version of FLake. Neglecting heating by solar radiation penetrating the ice cover did not introduce large errors in FLake applications to low-altitude, seasonally ice-covered lakes (Kirillin 2010; Bernhardt et al. 2012) where the incoming solar radiation in winter is lower and the relatively thick snow cover ~~dampen~~damps the radiative heating. However, in the high-altitude, low-latitude lakes of the Tibetan Plateau, the radiation penetrating the ice appears to be an important component of the lake heat budget, so

15   that the water temperatures directly after ice breakup are close to the maximum density value (Wen et al. 2016).

The water transparency characteristics used in the model configuration were adopted from (Kar 2014). The light extinction coefficient γ was calculated as the reciprocal of the Secchi depth h_S, $\gamma = C_\gamma h_S^{-1}$, assuming $C_\gamma = 1.8$, an approximate mid-value of the range reported in previous studies (see reviews in Kirillin and Shatwell 2016 and Shatwell et al. 2016).

Model performance was assessed by comparing daily averages of modeled and observed (in situ and satellite) surface

20   temperature (T_s) between May and October. The satellite data contained mostly only one data point on a given day, which may increase error. Some outliers existed usually under ice cover or subzero skin temperatures. All $T_s \leq 0$ were excluded from modeled and observed data, i.e. also the whole ice covered period. Different aspects of model performance were examined including model bias (Eq. 3), centred root mean square error ($RMSE_c$, Eq. 4), normalized standard deviation (σ_{norm}, Eq. 5), as well as normalized root mean square error (I_2 and I_3, Eq. 6 and 7).

25   $$bias = \bar{m} - \bar{o} \tag{3}$$

$$RMSE_c = \sqrt{\frac{1}{n} \sum_{i=1}^{n} ((m_i - \bar{m}) - (o_i - \bar{o}))^2} \tag{4}$$

$$\sigma_{norm} = \sqrt{\sum_{i=1}^{n} (m_i - \bar{m})^2 / \sum_{i=1}^{n} (o_i - \bar{o})^2} \tag{5}$$

$$\bar{-}I_2 = \sqrt{\frac{1}{n} \sum_{i=1}^{n} (o_i - m_i)^2} / \sqrt{\frac{1}{n} \sum_{i=1}^{n} o_i^2} \tag{6}$$

$$I_3 = \sqrt{\frac{1}{n} \sum_{i=1}^{n} (o_i - m_i)^2} / \sqrt{\frac{1}{n} \sum_{i=1}^{n} (o_i - \bar{o})^2} \tag{7}$$

30   Here m_i and o_i are the modeled and observed values, respectively, and $\bar{m}$ and $\bar{o}$ are their means.

7

2.7 Statistics and trend analysis.

The lakes were defined as stratified when the difference between surface and bottom temperature, $T_s - T_b > 0.5$ K for summer stratification, and $T_s - T_b < -0.5$ K or when the ice cover thickness $h_{ice} > 0$ for winter stratification. Stratification duration, as well as stratification start and end dates, given in day of the year (doy), refer to the longest uninterrupted stratification event each year/season. The lakes were defined as mixed when they were not stratified. Spring and autumn overturn were defined as the longest uninterrupted period of mixing following winter and summer stratification, respectively. In simulations, when the lakes froze in winter, they always remained frozen until thaw in spring. Therefore, the ice cover duration, as well as freeze and thaw dates, refer to both the longest uninterrupted period of ice cover and the total number of days of ice cover in each winter season. Seasons are defined from typical hydrological and ice regime as winter: Jan-Mar, Spring: Apr – Jun, Summer: Jul-Sep, Autumn: Oct-Dec. Trends in data were assessed using linear regressions. Homogeneity of variance and normality of residuals were assessed by inspecting plots of residuals vs fitted values and normal quantile-quantile plots. Leverage was assessed using Cook's distances. All statistical analyses were performed with R version 3.3.0 (R Core Team 2016). The satellite data on lake surface temperatures, despite the coverage of several decades, were found inappropriate for reliable trend estimation due to numerous data gaps of several months, exceeding the half-period of the seasonal variations (Fig. 3)

3. Results

3.1 Model performance

The model simulated the lake surface temperatures during the ice-free period well (Fig. 4, Table 1). The temperature bias of the model was negligible (<1% of the range of temperature variability) forced by both the NCEP and ERA reanalyses (Fig. 5). The correlation between modeled and observed values was notably high for the ERA input: $r = 0.96$, or 92% of variance captured by the model. The NCEP forcing provided slightly worse results: $r = 0.93$ or 86% of correctly simulated variance. The normalized standard deviation (σ_{norm}) was also better for the ERA forcing, differing from 1 by less than 0.3%, whereas σ_{norm} was around 1.25 for the NCEP input (Fig. 5).

Comparison of the model results to the satellite data demonstrated a slightly worse but still qualitatively acceptable agreement (Table 1, Fig. 3). Among obvious reasons for the disagreement is the low and irregular temporal resolution of the remote sensing data, as well as the differences between the surface temperatures in situ and the values derived empirically from remote infrared radiation measurements. The validation of the satellite data against the bulk in situ temperatures yielded similar divergences to the model-satellite comparison, indicating that the uncertainties in the satellite data were the primary reason for their deviation from the modeling results. The satellite data from the Pathfinder SST produced generally higher surface temperatures than both in situ data and modeling results, with the bias varying between 0.4 K for the three years of observations and 0.7-1.5 K for the 30 years of the modeling results (Table 1).

8

The strongest deviations of the model results from the in situ temperatures and remote sensing data were observed in the late spring and early summer (Figs. 2, 3). These deviations resulted apparently from the model uncertainties in the prediction of the ice cover breakup. No long-term time series on the ice breakup dates are available for the lakes of the region, making it impossible to quantify the model performance on the ice regime. An indirect estimation of the ice breakup dates from the surface temperatures in 2011-2013 suggests that the model error amounts to several weeks.

Since the model driven by the ERA data performed generally better than with the NCEP input, the results on seasonal characteristics and climatic trends are discussed below based on the ERA-FLake configuration. The outcomes of the NCEP-driven model were overall similar to those of the ERA-driven model with slightly higher water temperatures and weaker thermal stratification. The statistics are presented in Table 2, and an extended discussion of NCEP results is omitted for the sake of brevity.

3.2 Seasonal temperature and mixing regime

The modeled seasonal course of thermal stratification and ice regime was typical for a dimictic regime (Hutchinson 1975; Kirillin and Shatwell 2016) in both Tibetan lakes (Table 2). The ice-covered period lasted for 26-29 weeks and the ice thickness reached its maximum of 0.8-1.0 m in early March. Ice melted on 16 May +-1 week, followed by a 2-3 week period of full mixing (spring overturn). These phenological characteristics of the seasonal stratification were similar in Ngoring and Gyaring since they were not significantly affected by the differences in the morphology and water transparency. Both lakes stratified for 16-19 weeks in summer (Fig. 6). The autumn overturn (period of complete mixing) started around 14 Oct in Ngoring and about 3 weeks earlier in the shallower Gyaring. Autumn mixing also lasted longer in Gyaring, so that summer stratification was shorter. The full mixing period lasted 4-6 weeks, which is two times longer than the spring overturn - a remarkable feature of the seasonal mixing regime with important effects on the lake biogeochemistry as discussed below. The summer surface temperatures in Ngoring (12.01 °C) and Gyaring (12.16 °C) were similar. The temperatures at the lake bottom were in turn appreciably higher in shallower Gyaring (7.96 °C vs. 6.26 °C), which also implies generally higher mean temperatures in this lake. The differences in the water transparency between Ngoring and Gyaring were evident primarily in the thickness of the surface mixed layer h_{mix} (epilimnion) in summer: in Ngoring h_{mix} was 1.5-2.0 m deeper than in Gyaring (Fig. 7).

3.3 Trends in atmospheric forcing

Atmospheric forcing: The mean trends in the principal atmospheric variables differed in the NCEP and ERA reanalyses (Table 3). The ERA data showed significant trends only in air temperature (as warming at ~0.28°C per decade) and in air humidity. A positive humidity trend was present in the NCEP data too, whereas no trend existed in the air temperature. In turn, the NCEP data suggested a weak but statistically significant increase of cloud cover and a barely distinguishable decrease in wind speeds significant at ~97 % confidence level. The picture was clearer when the trends were split into seasonal bins: both reanalyses showed an increase in air temperatures in summer of 0.2-0.5°C per decade (with higher trend values in the ERA data). T_a, however, remained unchanged in spring and sank in autumn (statistically significant in NCEP only, at -0.5 °C per decade, and

9

insignificant in ERA at -0.15 °C per decade). The most significant increase of T_a occurred in winter (slightly stronger in ERA at 0.7°C per decade), resulting in a positive trend in annual T_a in the ERA data, but an insignificant trend in annual T_a in the NCEP data. The decrease in the solar radiation in summer, as the major driver of the regional heat budget, was remarkable in both datasets (-3.8 W m^{-2} decade^{-1} in ERA vs -1.2 W m^{-2} decade^{-1} in NCEP).

3.4 Long-term lake response to atmospheric trends

Several characteristics of the seasonal thermal regime did not reveal any significant long-term trends in either of the two lakes based on model simulations with both reanalysis datasets. These characteristics included the dates of onset and breakup of the ice cover, ice thickness, dates of full mixing in spring, dates of the maximum ice thickness and of the maximum surface temperature, bottom temperature and mean lake temperatures in summer. The fact that mean water temperature remained essentially unaffected by long-term atmospheric trends in both lakes is rather unexpected in view of the numerous reports on lake warming throughout the world. In the ERA-driven results, the surface temperature, T_s, did not increase significantly in either lake, whereas according to the NCEP reanalysis, T_s increased at 0.24°C per decade and 0.18°C per decade in Ngoring and Gyaring, respectively (Table 4).

There were marginally insignificant signs of an increase in stratification and decrease in mixing across the lake water column in Ngoring, but not in Gyaring, under NCEP forcing, including a weak decrease of the mixed layer depth (0.27 m decade^{-1}, significance level 0.06 only) accompanied by a decrease in the deep water temperatures (0.29 K decade^{-1}, p=0.10). Also the increase in T_s was slightly weaker in Gyaring (0.18 K decade^{-1} vs. 0.24 K decade^{-1} in Ngoring).

4 Discussion

4.1 Model performance

FLake demonstrated good abilities to capture the thermal characteristics of high-altitude lakes. In particular, the good simulation of the surface temperature indicates that the model is suitable for lake representation in coupled land-atmosphere modeling of the Tibetan Plateau and other alpine regions. The performance of the model for the two Tibetan lakes is comparable to that reported previously in temperate (Kirillin 2010; Stepanenko et al. 2014; Shatwell et al. 2016) and tropical (Thiery et al. 2014) lakes. The results underscore the importance of the atmospheric input for the correct simulation of lake thermodynamics: The ERA Interim—a more recent reanalysis dataset with updated data assimilation—provides an appreciably better FLake output, while the older generation NCEP/NCAR dataset demonstrates an appreciable bias in lake temperatures as well as slightly higher root-mean-square error. A better performance of the ERA reanalyses over the Tibetan highlands, in particular, in reproducing the observed long-term trends in air temperature, has been also reported in earlier studies (Bao and Zhang 2013).

The major drawback of the model, which should be taken into account when simulating the thermal regime of Tibetan lakes, as well as other high-altitude lake systems with an extended ice-covered season and low snow precipitation in winter, is an

oversimplified representation of the winter conditions during the ice-covered period. The performance of FLake at simulating ice cover in temperate freshwater lakes was previously analyzed by Bernhardt et al. (2012). FLake, as well as all other lake parameterization schemes currently used in land-atmosphere coupling of climate models (Hostetler et al. 1993; Subin et al. 2012), neglects heating of the water column by solar radiation penetrating the ice cover. One of the negative effects of this

5 simplification is the error in simulating the ice thickness and the ice breakup date. It was not possible to quantitatively estimate this effect in the present study due to the lack of long-term observations on ice-on and ice-off dates. Nevertheless, the modeled duration of the ice cover from October-November to May-June and the ~1 m maximal ice thickness in Tibetan lakes agree with the existing occasional field observations (Wen et al. 2016). The modeling results on the ice thickness may be assumed more reliable than ice break-up dates since ice growth is mainly governed by the ice-atmosphere heat budget (Aslamov et al.

10 2014; Leppäranta 2015), which is well captured by the model. Another apparent error introduced by neglecting the under-ice radiative heating is that the mean heat content of the lake after ice-off is underestimated. The result is a strong underestimation of the lake surface temperatures in early summer. ~Taking into account strong constraints on the computational costs of the lake parameterization schemes, a remarkable improvement in regional climate models can be achieved by extending the lake modules to include one of the bulk algorithms developed earlier for convective mixing based on integration across the mixed

15 layer of the equation for mixing energy production with solar radiation as a volumetric energy source (Mironov et al. 2002; Oveisy and Boegman 2014).

Taking into account strong constraints on the computational costs of the lake parameterization schemes, a remarkable improvement in regional climate models can be achieved by extending the lake modules to include one of the integrated bulk algorithms of solar heating and convective mixing developed earlier (Mironov et al. 2002; Oveisy and Boegman 2014).

20 The surface temperatures provided by the AVHRR Pathfinder product were generally higher than both in situ and modeled temperatures. The reason for the positive bias is not clear: we may tentatively relate the error to an overestimation of the cool skin effect by the current AVHRR algorithm and hypothesize that corrections for the atmospheric radiation, used in the empirical Pathfinder SST algorithms do not perform well over high-mountain regions with low atmospheric density/radiation. The cool skin effect, while not considered directly in our study, is however expected to be even stronger in high-altitude lakes

25 than in the ocean, due to strong radiative heating and permanent cooling at the lake surface (Li et al. 2015).

4.2 Seasonal thermal regime and ice conditions

Both studied lakes are clearly dimictic and share the typical features of this type of mixing regime found in other regions: two periods of weak vertical mixing lasting several months separated by shorter periods of full vertical mixing (overturns) in spring and in autumn. As follows from the modeling results, a particular difference of the dimictic regime in Tibetan lakes from those

30 in lowland temperate regions is the comparably short period of spring overturn (SO), so that summer stratification forms only about one week after ice-off. This is apparently due to the alpine climatic conditions, where the low air temperatures produce relatively long ice-covered periods, which last until late May or early June. The solar radiation flux in the early summer is however much stronger than at lower altitudes and quickly heats the upper water column directly after ice-off.

11

Since spring overturn was short, the major biogeochemical processes that take place when oxygenated surface water comes into contact with the highly mineralized sediment should occur in autumn, when overturn is longer. The characteristics of biogeochemical processes in Tibetan lakes are largely unknown, but some key features, in particular, the oxygen regime, may be deduced from the seasonal stratification pattern (Golosov et al. 2007). Due to the low eutrophication of both lakes, oxygen consumption rates are probably low. Strong vertical oxygen gradients and an oxygen deficit in the deep parts of the lakes probably develop during ice-covered periods, when the lake surface is isolated from the atmosphere for several months. This oxygen deficit in turn may trigger biogeochemical processes at the interface between the water and the highly mineralized lake sediment, such as methane production. The spring overturn may be too short to completely replenish the depleted oxygen after winter, so that the anoxic conditions may persist in the deep layers of lakes throughout the summer season, isolated by the stratification. In this case, the most intensive exchange between the lake hypolimnion and the atmosphere, including potential emissions of methane and carbon dioxide should most probably appear during the autumn overturn.

4.3 Lake response to climatic trends in external forcing

Surface temperatures of lakes are recognized as important indicators of regional climate change driven by global warming (Adrian, others). In temperate climate regions, warming trends in lakes are reported to be close to the air temperature trends (Arhonditsis et al. 2004; Danis et al. 2004; Kirillin 2010; Schneider and Hook 2010). Some studies even suggest that temperate lakes warm faster than the atmosphere due to shortening of the ice covered period and, as a result, higher storage of incoming solar radiation (Austin and Colman 2007; Kintisch 2015). On the other hand, tropical and alpine lakes tend to warm more slowly than the air above (Livingstone 2003; Vollmer et al. 2005; Coats et al. 2006). A recent synthesis of available lake temperature data (O'Reilly et al. 2015) has revealed high geographic variability in lake warming trends over the globe. In particular, no significant warming trends were determined for lakes on the Tibetan Plateau. Our results indeed suggest that Tibetan lakes have not been warming during the last several decades and provide insight into the mechanisms behind this.

Atmospheric warming trends were present in both reanalysis datasets, although these were unevenly distributed over the seasons. Air temperature increased in summer (more strongly in the ERA reanalysis at 0.5 K decade^{-1} than in NCEP at 0.2 K decade^{-1}), remained unchanged in spring, decreased in autumn (significantly only in NCEP at -0.5 K decade^{-1}, and insignificantly in ERA at -0.15 K decade^{-1}), and increased in winter (slightly more in ERA at +0.7 K decade^{-1} vs +0.4 K decade^{-1} in NCEP). The winter warming trend was stronger than the summer trend, but its effect on lakes is weak due to isolation from the atmosphere by the ice cover. The statistically significant but rather small tendency for ice thickness to decrease at ~1 cm decade^{-1} simulated in both Ngoring and Gyaring may be related to the overall effect of a warmer atmosphere in winter.

Despite the overall warming of the atmosphere, which was especially apparent in the ERA dataset, there was no significant trend in the lake surface temperatures in the ERA-forced results, and only a slight increasing trend in the NCEP results. This fact is closely connected to the negative trend in the solar radiation, which decreased in the ERA dataset at 3.8 Wm^{-2} decade^{-1}, more than 3 times faster than in the NCEP dataset. A characteristic feature of Tibetan lakes as compared with lowland lakes is their stronger heating by solar radiation and, as a result, a persistently warmer lake surface than the atmosphere (Wen et al.

12

2016). Hence, the effects of the air temperature increase on the lake heat budget were counteracted by the reduced radiative heating, resulting in no significant long term change of the mean lake temperatures (Fig. 8). This core result of the present study indicates that trends in the lake temperatures are not coupled directly to the increase of the air temperature and underscores the crucial role of short-wave radiation for thermal conditions in alpine lakes.

5   In general, the response of the stratification regime to changes in external atmospheric forcing in deep and clear Ngoring was stronger than in shallow and more turbid Gyaring, which was most apparent in the NCEP-forced results. A plausible explanation of this effect is that the high turbidity of the Gyaring water ~~dampen~~damped the effects of higher air temperatures and weaker solar radiation. In the transparent waters of Ngoring, the effect of the radiation decrease is distributed over a water column several meters thick, whereas the increase of the air temperature affects the heat transport at the upper air-water

10   interface. This decoupling of the two counteracting trends produced a temperature increase at the upper boundary with a simultaneous decrease of the heat content in the water column beneath, resulting in a shallower mixed layer and stronger stratification, as found in the modeling results for Ngoring, but not for Gyaring (see Results). In Gyaring, on the other hand, both the decrease in radiation and the increase in air temperature are concentrated at the lake surface: the daytime heat is stored in a shallower surface layer, and is more quickly released to the atmosphere by night-time cooling. Thus, the opposing trends

15   in air temperature and radiation effectively cancel each other at the lake surface with little effect on the thermal characteristics of deeper waters.

To quantify the counteracting effects of the ~~growing~~increasing air temperature and the decreasing short-wave radiation, we performed model runs using artificial short-wave radiation input constructed from ERA values (which had a significant negative trend) with the summer radiation trend removed. The trend was removed based on daily averaged values, and the

20   diurnal cycle of solar radiation was subsequently restored to the detrended values based on daytime duration and the daily maximum~~ums~~a of solar radiation. Additionally, a 'control' model run was performed with the radiation input reconstructed from daily averages using the same procedure, but without trend removal. The model results based on the modified 'control' radiation input did not differ significantly from those based on the original ERA input (not shown). In turn, the model driven by the detrended radiation input produced a positive trend in the mean summer surface temperature of 0.26 °C decade^{-1} and

25   the maximum summer surface temperature of 0.34 °C decade^{-1}. The trend in surface water temperatures was significant at > 99% level of confidence (p = 0.003), whereas the original ERA input produced no significant long-term increase of surface temperatures (0.15 °C decade^{-1} at < 93% level of confidence, see Table 4). Hence, the short-wave radiation decrease did indeed cancel the effect of the air temperature increase on lake temperatures ~~caused the cancellation of the lake warming~~ in ERA-driven scenarios. The hypothetical surface temperature trend 0.26 °C decade^{-1} is still lower than the summer air temperature

30   increase of 0.50 °C decade^{-1}, and is accompanied by significant changes in the summer stratification: a later breakdown of the stratification due to autumn cooling (1.8 days decade^{-1}, p = 0.034) and a shallower surface mixed layer depth (0.14 m decade^{-1}, p = 0.006). Several previous studies devoted to ~~the~~ alpine or tropical lakes also reported lake temperature trends lower than the regional atmosphere warming (Livingstone 2003; Vollmer et al. 2005; Coats et al. 2006), while lowland temperate lakes are often found to be in a thermal equilibrium with the atmosphere (Arhonditsis et al. 2004; Danis et al. 2004; Kirillin 2010).

13

:

The radiation decrease can be hypothetically related to the direct effect of anthropogenic aerosols at high altitudes. Another possible reason for the lower solar radiation flux in the Tibetan highlands might be increased evaporation, and as a result, higher air humidity, which is also supported by positive trends in the humidity and cloud amount present in reanalysis data. In particular, Shen et al. (2015) report local cooling over the Tibetan Plateau due to increased evaporation resulting from increased vegetation growth. The exact mechanisms of the decrease of the solar radiation of the Tibetan Plateau require further investigation. Our model experiments are well supported by the observational data from the largest freshwater lake of the Tibetan Plateau, and involve comparison of lake They compare the dynamics of lakes with different depths and water transparencies under the same atmospheric forcing, characteristic for high-altitude conditions. By this, tThe presented results provide the first detailed insight into the specific mechanisms of internal lake mixing and lake-atmosphere coupling, specific forto the Tibetan lakes and extendable onto other high-altitude hydrological systems. It should be noted that freshwater lakes comprise only about 10% of the Tibetan lake system (Jiang and Huang 2004), while ~75% of lakes have brackish or saline water (the salt content of the rest of lakes is unknown). The salt stratification can significantly contribute to the seasonal mixing regime as well as to the lake response to long-term changes in the atmospheric input. Effects of salinity, as well as lake physics during the ice-covered period, as discussed above, are the two major facets of lake dynamics for further clarification with regard to specific features of the Tibetan lake system.

Author contribution

GK conceived and designed the study, and performed modelling and analysis of the remote sensing data. LW performed collection and analysis of field measurements. TS evaluated the model performance and performed statistical trend analysis. All authors contributed to the final analysis of results. GK and TS wrote the ms with contributions from LW.

Competing interests

The authors declare that they have no conflict of interest.

Acknowledgements

14

References

Arhonditsis, G. B., M. T. Brett, C. L. DeGasperi, and D. E. Schindler. 2004. Effects of Climatic Variability on the Thermal Properties of Lake Washington. Limnol. Oceanogr. **49**: 256–270.

Aslamov, I. A., V. V. Kozlov, G. B. Kirillin, I. B. Mizandrontsev, K. M. Kucher, M. M. Makarov, A. Y. Gornov, and N. G. Granin. 2014. Ice–water heat exchange during ice growth in Lake Baikal. J. Gt. Lakes Res. **40**: 599–607.

Austin, J. A., and S. M. Colman. 2007. Lake Superior summer water temperatures are increasing more rapidly than regional air temperatures: A positive ice-albedo feedback. Geophys. Res. Lett. **34**.

Bao, X., and F. Zhang. 2013. Evaluation of NCEP–CFSR, NCEP–NCAR, ERA-Interim, and ERA-40 reanalysis datasets against independent sounding observations over the Tibetan Plateau. J. Clim. **26**: 206–214.

Bernhardt, J., C. Engelhardt, G. Kirillin, and J. Matschullat. 2012. Lake ice phenology in Berlin-Brandenburg from 1947-2007: observations and model hindcasts. Clim. Change **112**: 791–817. doi:10.1007/s10584-011-0248-9

Biermann, T., W. Babel, W. Ma, X. Chen, E. Thiem, Y. Ma, and T. Foken. 2014. Turbulent flux observations and modelling over a shallow lake and a wet grassland in the Nam Co basin, Tibetan Plateau. Theor. Appl. Climatol. **116**: 301–316.

Casey, K. S., T. B. Brandon, P. Cornillon, and R. Evans. 2010. The Past, Present, and Future of the AVHRR Pathfinder SST Program, p. 273–287. *In* V. Barale, J.F.R. Gower, and L. Alberotanza [eds.], Oceanography from Space. Springer Netherlands.

Cheng, G., and T. Wu. 2007. Responses of permafrost to climate change and their environmental significance, Qinghai-Tibet Plateau. J. Geophys. Res. Earth Surf. **112**.

Coats, R., J. Perez-Losada, G. Schladow, R. Richards, and C. Goldman. 2006. The Warming of Lake Tahoe. Clim. Change **76**: 121–148. doi:10.1007/s10584-005-9006-1

Dai, Y., T. Yao, X. Li, and F. Ping. 2016. The impact of lake effects on the temporal and spatial distribution of precipitation in the Nam Co basin, Tibetan Plateau. Quat. Int.

Danis, P.-A., U. von Grafenstein, V. Masson-Delmotte, S. Planton, D. Gerdeaux, and J.-M. Moisselin. 2004. Vulnerability of two European lakes in response to future climatic changes. Geophys. Res. Lett. **31**: 21507.

Dee, D. P., S. M. Uppala, A. J. Simmons, and others. 2011. The ERA-Interim reanalysis: configuration and performance of the data assimilation system. Q. J. R. Meteorol. Soc. **137**: 553–597. doi:10.1002/qj.828

Dutra, E., V. M. Stepanenko, G. Balsamo, P. Viterbo, P. Miranda, D. Mironov, and C. Schär. 2010. An offline study of the impact of lakes in the performance of the ECMWF surface scheme. Boreal Environ. Res. **15**.

Gerken, T., W. Babel, F. Sun, M. Herzog, Y. Ma, T. Foken, and H.-F. Graf. 2013. Uncertainty in atmospheric profiles and its impact on modeled convection development at Nam Co Lake, Tibetan Plateau. J. Geophys. Res. Atmospheres **118**.

15

Golosov, S., and G. Kirillin. 2010. A parameterized model of heat storage by lake sediments. Environ. Model. Softw. **25**: 793–801. doi:10.1016/j.envsoft.2010.01.002

Golosov, S., O. Maher, E. Schipunova, A. Terzhevik, G. Zdorovennova, and G. Kirillin. 2007. Physical background of the development of oxygen depletion in ice-covered lakes. Oecologia **151**: 331–340. doi:10.1007/s00442-006-0543-8

Gu, S., Y. Tang, X. Cui, T. Kato, M. Du, Y. Li, and X. Zhao. 2005. Energy exchange between the atmosphere and a meadow ecosystem on the Qinghai–Tibetan Plateau. Agric. For. Meteorol. **129**: 175–185.

Haginoya, S., H. Fujii, T. Kuwagata, J. Xu, Y. Ishigooka, S. Kang, and Y. Zhang. 2009. Air-lake interaction features found in heat and water exchanges over Nam Co on the Tibetan Plateau. Sola **5**: 172–175.

Hostetler, S. W., G. T. Bates, and F. Giorgi. 1993. Interactive coupling of a lake thermal model with a regional climate model. J. Geophys. Res. Atmospheres **98**: 5045–5057.

Hutchinson, G. E. 1975. A treatise on limnology: Geography, physics, and chemistry. Chemistry of lakes, Wiley.

Jiang, J., and Q. Huang. 2004. Distribution and variation of lakes in Tibetan Plateau and their comparison with lakes in other part of China. Water Resour. Prot. **4**: 24–27.

Kalnay, E., M. Kanamitsu, R. Kistler, and others. 1996. The NCEP/NCAR 40-year reanalysis project. Bull. Am. Meteorol. Soc. **77**: 437–471.

Kar, D. 2014. Wetlands and Lakes of the World, 2014 edition. Springer.

Kintisch, E. 2015. Earth's lakes are warming faster than its air. Science **350**: 1449–1449.

Kirillin, G. 2010. Modelling the impact of global warming on water temperature and seasonal mixing regimes in small temperate lakes. Boreal Env. Res **15**: 279–293.

Kirillin, G., J. Hochschild, D. Mironov, A. Terzhevik, S. Golosov, and G. Nützmann. 2011. FLake-Global: Online lake model with worldwide coverage. Environ. Model. Softw. **26**: 683–684.

Kirillin, G., and T. Shatwell. 2016. Generalized scaling of seasonal thermal stratification in lakes. Earth-Sci. Rev. **161**: 179–190.

Leppäranta, M. 2015. Freezing of Lakes and the Evolution of their Ice Cover, Springer Berlin Heidelberg.

Li, M., Y. Ma, Z. Hu, H. Ishikawa, and Y. Oku. 2009. Snow distribution over the Namco lake area of the Tibetan Plateau. Hydrol. Earth Syst. Sci. **13**: 2023–2030.

Li, Z., S. Lyu, Y. Ao, L. Wen, L. Zhao, and S. Wang. 2015. Long-term energy flux and radiation balance observations over Lake Ngoring, Tibetan Plateau. Atmospheric Res. **155**: 13–25.

Li, Z., S. Lyu, L. Zhao, L. Wen, Y. Ao, and S. Wang. 2016. Turbulent transfer coefficient and roughness length in a high-altitude lake, Tibetan Plateau. Theor. Appl. Climatol. **124**: 723–735.

Lin, Z., F. Niu, H. Liu, and J. Lu. 2011. Hydrothermal processes of alpine tundra lakes, Beiluhe basin, Qinghai-Tibet Plateau. Cold Reg. Sci. Technol. **65**: 446–455.

Liu, J., S. Wang, S. Yu, D. Yang, and L. Zhang. 2009. Climate warming and growth of high-elevation inland lakes on the Tibetan Plateau. Glob. Planet. Change **67**: 209–217.

16

Livingstone, D. M. 2003. Impact of Secular Climate Change on the Thermal Structure of a Large Temperate Central European Lake. Clim. Change **57**: 205–225. doi:10.1023/A:1022119503144

Ma, Y., B. Wang, L. Zhong, and W. Ma. 2012. The regional surface heating field over the heterogeneous landscape of the Tibetan Plateau using MODIS and in-situ data. Adv. Atmospheric Sci. **29**: 47–53.

Ma, Y., Y. Wang, R. Wu, and others. 2009. Recent advances on the study of atmosphere-land interaction observations on the Tibetan Plateau. Hydrol. Earth Syst. Sci. **13**: 1103–1111.

Mallard, M. S., C. G. Nolte, O. R. Bullock, T. L. Spero, and J. Gula. 2014. Using a coupled lake model with WRF for dynamical downscaling. J. Geophys. Res. Atmospheres **119**: 7193–7208.

Mironov, D. 2008. Parameterization of lakes in numerical weather prediction. Description of a lake model. 11. 11 Deutscher Wetterdienst.

Mironov, D., B. Ritter, J.-P. Schulz, M. Buchhold, M. Lange, and E. Machulskaya. 2012. Parameterisation of sea and lake ice in numerical weather prediction models of the German Weather Service. Tellus A **64**.

Mironov, D., A. Terzhevik, G. Kirillin, T. Jonas, J. Malm, and D. Farmer. 2002. Radiatively driven convection in ice-covered lakes: Observations, scaling, and a mixed layer model. J. Geophys. Res. **107**: 3032.

Niiler, P. P., and É. Kraus. 1979. One-dimensional models of the upper layer of the ocean, p. 175–208. *In* Modeling and Prediction of the Upper Layers of the Ocean. Pergamon.

O'Reilly, C. M., S. Sharma, D. K. Gray, and others. 2015. Rapid and highly variable warming of lake surface waters around the globe. Geophys. Res. Lett. **42**.

Oveisy, A., and L. Boegman. 2014. One-dimensional simulation of lake and ice dynamics during winter. J. Limnol. **73**.

R Core Team. 2016. R: A language and environment for statistical computing. R Foundation for Statistical Computing, Vienna, Austria. 2015. URL h ttp. Www R-Proj. Org.

Rooney, G. G., and I. D. Jones. 2010. Coupling the 1-D lake model FLake to the community land-surface model JULES. Boreal Environ. Res. **15**: 501–512.

Salgado, R., and P. Le Moigne. 2010. Coupling of the FLake model to the Surfex externalized surface model. Boreal Environ. Res. **15**: 231–244.

Schneider, P., and S. J. Hook. 2010. Space observations of inland water bodies show rapid surface warming since 1985. Geophys. Res. Lett. **37**.

Shatwell, T., R. Adrian, and G. Kirillin. 2016. Planktonic events may cause polymictic-dimictic regime shifts in temperate lakes. Sci. Rep. **6**.

Shen, M., S. Piao, S.-J. Jeong, and others. 2015. Evaporative cooling over the Tibetan Plateau induced by vegetation growth. Proc. Natl. Acad. Sci. **112**: 9299–9304.

Stepanenko, V., K. D. Jöhnk, E. Machulskaya, M. Perroud, Z. Subin, A. Nordbo, I. Mammarella, and D. Mironov. 2014. Simulation of surface energy fluxes and stratification of a small boreal lake by a set of one-dimensional models. Tellus A **66**.

Su, F., L. Zhang, T. Ou, D. Chen, T. Yao, and K. Tong. 2015. Hydrological response to future climate changes for the major upstream river basins in the Tibetan Plateau. ResearchGate **136**. doi:10.1016/j.gloplacha.2015.10.012

Subin, Z. M., W. J. Riley, and D. Mironov. 2012. An improved lake model for climate simulations: model structure, evaluation, and sensitivity analyses in CESM1. J. Adv. Model. Earth Syst. **4**.

Sun, S., J. Yan, N. Xia, and C. Sun. 2007. Development of a model for water and heat exchange between the atmosphere and a water body. Adv. Atmospheric Sci. **24**: 927–938.

Thiery, W., V. M. Stepanenko, X. Fang, and others. 2014. LakeMIP Kivu: evaluating the representation of a large, deep tropical lake by a set of one-dimensional lake models. Tellus A **66**.

Vollmer, M. K., H. A. Bootsma, R. E. Hecky, G. Patterson, J. D. Halfman, J. M. Edmond, D. H. Eccles, and R. F. Weiss. 2005. Deep-Water Warming Trend in Lake Malawi, East Africa. Limnol. Oceanogr. **50**: 727–732.

Wang, M., J. Hou, and Y. Lei. 2014. Classification of Tibetan lakes based on variations in seasonal lake water temperature. Chin. Sci. Bull. **59**: 4847–4855. doi:10.1007/s11434-014-0588-8

Wen, L., S. Lv, Z. Li, L. Zhao, and N. Nagabhatla. 2015. Impacts of the Two Biggest Lakes on Local Temperature and Precipitation in the Yellow River Source Region of the Tibetan Plateau. Adv. Meteorol. **2015**.

Wen, L., S. Lyu, G. Kirillin, Z. Li, and Z. Lin. 2016. Air-Lake Boundary Layer and performance of a simple lake parameterization scheme ovr the Tibetan Highlands. Tellus A

Xu, J., S. Yu, J. Liu, S. Haginoya, Y. Ishigooka, T. Kuwagata, M. Hara, and T. Yasunari. 2009. The implication of heat and water balance changes in a lake basin on the Tibetan Plateau. Hydrol. Res. Lett. **3**: 1–5.

Yang, K., H. Wu, J. Qin, C. Lin, W. Tang, and Y. Chen. 2014. Recent climate changes over the Tibetan Plateau and their impacts on energy and water cycle: A review. Glob. Planet. Change **112**: 79–91.

Yang, M., F. E. Nelson, N. I. Shiklomanov, D. Guo, and G. Wan. 2010. Permafrost degradation and its environmental effects on the Tibetan Plateau: A review of recent research. Earth-Sci. Rev. **103**: 31–44.

Yang, X., Y. Lü, Y. Ma, and J. Wen. 2015. Summertime thermally-induced circulations over the Lake Nam Co region of the Tibetan Plateau. J. Meteorol. Res. **29**: 305–314.

Zhang, G., T. Yao, H. Xie, S. Kang, and Y. Lei. 2013. Increased mass over the Tibetan Plateau: from lakes or glaciers? Geophys. Res. Lett. **40**: 2125–2130.

Zhang, G., T. Yao, H. Xie, J. Qin, Q. Ye, Y. Dai, and R. Guo. 2014. Estimating surface temperature changes of lakes in the Tibetan Plateau using MODIS LST data. J. Geophys. Res. Atmospheres **119**: 8552–8567.

Zheng, M. 2011. Resources and eco-environmental protection of salt lakes in China. Environ. Earth Sci. **64**: 1537–1546.

18

Tables

Table 1: Goodness of fit statistics for simulations in Ngoring and Gyaring based on surface temperatures. Simulations were forced by either the ERA-Interim or the NCEP/NCAR reanalyses. The last row shows a comparison of satellite-derived surface temperatures with in-situ measurements in Ngoring. Statistics are described in the methods (Eq. 3 – 7).

Lake	Forcing	Reference data	Bias (K)	*RMSE* (K)	*RMSE$_c$* (K)	I_2	I_3	σ_{norm}
Ngoring	**NCEP**	**in-situ**	**0.24**	**2.07**	**1.62**	**0.15**	**0.42**	**1.25**
Ngoring	**ERA**	**in-situ**	**0.11**	**1.11**	**1.10**	**0.10**	**0.29**	**1.00**
Ngoring	NCEP	satellite	-0.77	2.12	1.98	0.21	0.54	1.25
Ngoring	ERA	satellite	-0.70	1.87	1.73	0.18	0.48	1.03
Gyaring	NCEP	satellite	-1.47	3.17	2.81	0.32	0.87	1.48
Gyaring	ERA	satellite	-1.42	2.47	2.01	0.25	0.67	1.22
Ngoring	**In situ**	**satellite**	**-0.39**	**2.49**	**2.73**	**0.25**	**0.64**	**0.77**

5

19

Table 2: Mean characteristics of the seasonal thermal regime in Ngoring and Gyaring forced by the NCEP/NCAR and ERA-Interim reanalysis datasets. T_s, T_b, and T_m are temperatures at the surface, bottom, and averaged over the whole water column, respectively; h_{mix} and h_{ice} are the thickness of the mixed layer and the ice cover respectively; doy is day of the year.

| Variable	Units	Ngoring NCEP		Ngoring ERA		Gyaring NCEP		Gyaring ERA	
		mean	sd	mean	sd	mean	sd	mean	sd
Maximum T_s	°C	15.6	1.1	14.1	0.8	16.5	1.2	15.1	0.9
Timing of maximum T_s	doy	222.2	10.8	220.1	9.8	212.2	13.5	211.0	14.0
Stratification duration	d	113.6	15.9	134.6	12.9	81.6	32.2	115.5	14.6
Stratification start	doy	165.1	10.6	153.3	8.2	167.8	15.0	151.3	8.0
Stratification end	doy	278.8	7.4	287.9	6.2	251.3	16.9	266.7	9.2
Winter stratification duration	d	196.3	6.0	180.6	10.0	203.8	7.3	186.0	9.7
Total Ice duration	d	189.9	5.6	173.0	9.2	200.4	6.1	182.7	9.9
Freeze time	doy	-45.9	3.1	-35.2	5.5	-55.7	4.0	-44.3	5.3
Thaw time	doy	142.6	4.9	136.5	7.6	143.2	4.9	137.0	7.5
Maximum h_{ice}	m	1.0	0.04	0.8	0.04	1.0	0.04	0.9	0.04
Timing of maximum h_{ice}	doy	68.8	7.2	57.9	10.0	67.0	6.2	56.1	11.4
Spring overturn duration	d	22.0	11.0	16.3	9.0	20.1	12.4	13.1	8.9
Spring overturn start	doy	142.6	4.9	136.5	7.6	143.7	5.3	138.8	8.3
Spring overturn end	doy	163.7	10.5	152.3	8.2	166.1	13.7	150.2	7.9
Autumn overturn duration	d	30.9	8.9	31.1	8.6	52.2	19.5	46.9	11.4
Autumn overturn start	doy	279.2	7.0	288.0	6.1	251.1	18.4	267.2	10.3
Autumn overturn end	doy	310.1	3.6	319.1	4.1	303.3	3.9	314.1	4.4
T_s (summer mean)	°C	12.8	0.7	12.0	0.5	13.1	0.6	12.2	0.5
T_m (summer mean)	°C	10.4	0.5	9.2	0.5	11.7	0.8	10.2	0.7
T_b (summer mean)	°C	7.3	1.3	6.3	1.0	9.7	1.7	8.0	1.1
h_{mix} (summer mean)	m	7.5	1.0	5.6	0.5	5.6	1.2	3.8	0.6
h_{ice} (winter mean)	m	0.9	0.03	0.8	0.04	0.9	0.03	0.8	0.04

5

Table 3: Comparison of meteorological variables in the ERA and NCEP reanalysis datasets. I_R : incoming solar radiation [W m^{-2}], T_a : 2-m air temperature [°C], e_a : 2-m air humidity [mb], U_{10} : 10-m wind speed [m s^{-1}], N : total cloud cover [0-1]. Trends are given in units of the variable per year when significant at $p < 0.05$ (*), $p < 0.01$ (**) and $p < 0.001$ (***).

Variable	ERA			NCEP		
	Mean	**sd**	**Trend**	**Mean**	**sd**	**Trend**
Annual						
I_R	191.97	3.75		179.25	1.61	
T_a	-4.47	0.63	**0.0282****	-5.59	0.49	
e_a	3.30	0.18	**0.0085****	6.34	0.38	**0.0156****
U_{10}	4.01	0.11		4.98	0.20	**-0.0060***
N	0.57	0.03		0.32	0.02	**0.0008****
Winter						
I_R	167.63	2.35		152.07		
T_a	-13.11	1.49	**0.0696****	-16.19	1.45	**0.0486***
e_a	1.09	0.11		2.77	0.21	**0.0095*****
U_{10}	5.11	0.38		5.72		
N	0.58	0.05		0.24	0.03	**0.0009***
Spring						
I_R	247.25	6.62		232.41	2.84	
T_a	0.46	0.58		0.18	0.68	
e_a	4.03	0.28		7.91	0.58	**0.0194***
U_{10}	3.76	0.16		4.96	0.27	**-0.0089***
N	0.67	0.04	**0.0013***	0.42	0.03	
Summer						
I_R	204.80	10.26	**-0.3824***	204.39	4.36	**-0.1196***
T_a	4.74	0.84	**0.0504*****	6.09	0.71	**0.0248****
e_a	6.41	0.48	**0.0262*****	11.03	1.06	**0.0314***
U_{10}	2.98	0.13		4.21		
N	0.61	0.05		0.43		
Autumn						
I_R	148.35	3.68		128.21	1.40	**0.0468***
T_a	-10.08	1.00		-12.58	1.03	**-0.0460****
e_a	1.63	0.17		3.59	0.24	
U_{10}	4.22	0.32		5.03	0.35	
N	0.43	0.05		0.22	0.03	**0.0010***

5

Table 4: Trends in characteristics of the lake thermal regime. Abbreviations as for Table 2.

Variable	Units (per year)	Ngoring NCEP Trend	p	Ngoring ERA Trend	p	Gyaring NCEP Trend	p	Gyaring ERA Trend	p
Maximum T_s	°C	**0.032***	*0.023*						
Stratification duration	d	**0.492***	*0.022*						
Stratification start	doy	*-0.274*	*0.058*						
Stratification end	doy	**0.218***	*0.029*						
Winter stratification duration	d							**-0.376***	*0.023*
Maximum h_{ice}	m	**-0.001***	*0.034*			**-0.001***	*0.031*	**-0.001***	*0.037*
Autumn overturn duration	d	**-0.338****	*0.004*						
Autumn overturn start	doy	**0.216***	*0.021*						
Autumn overturn end	doy	**-0.122***	*0.012*						
T_s (summer mean)	°C	**0.024***	*0.012*	*0.015*	*0.071*	**0.018***	*0.033*		
h_{mix} (summer mean)	m	*-0.027*	*0.057*						

22

Figures
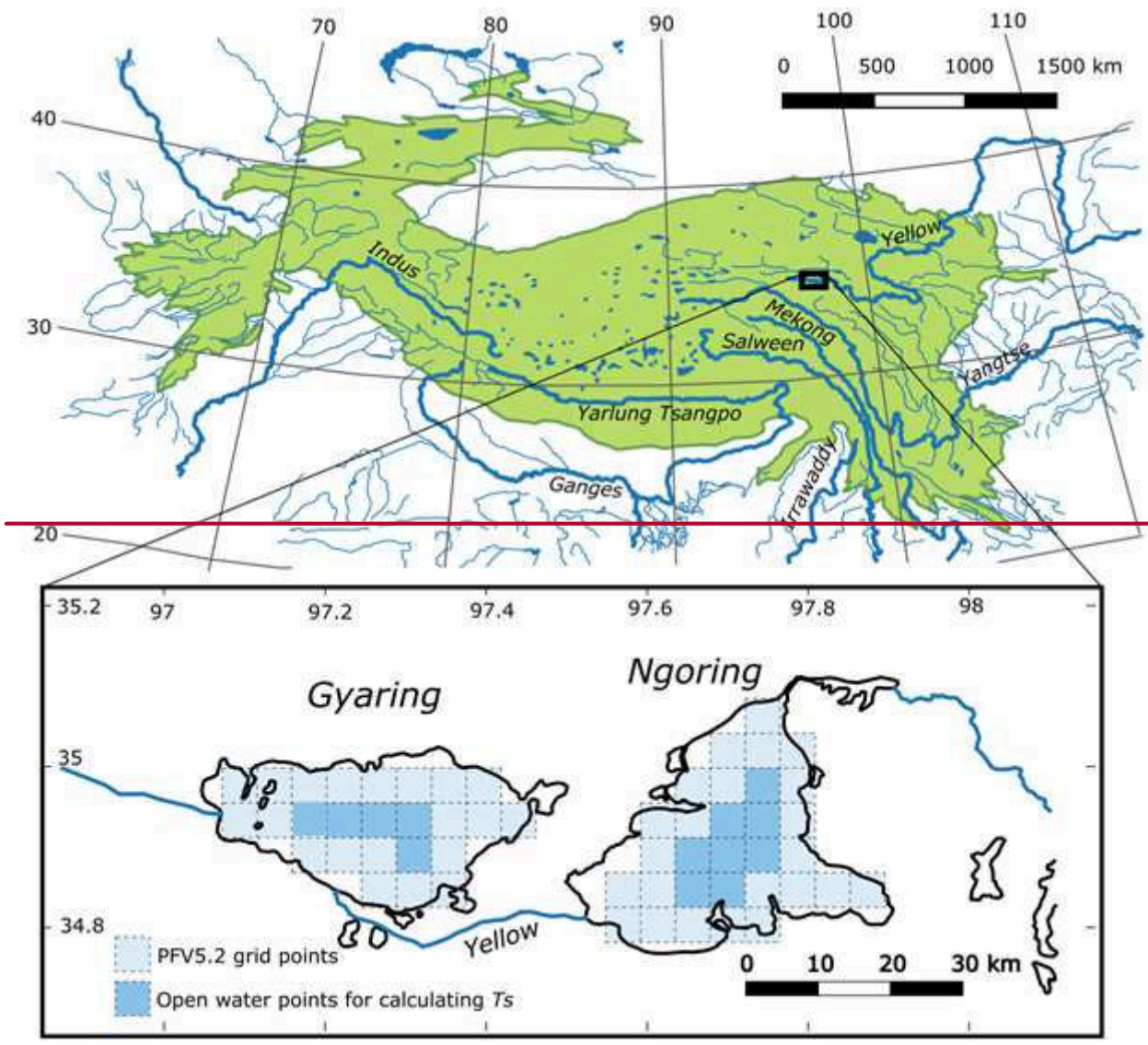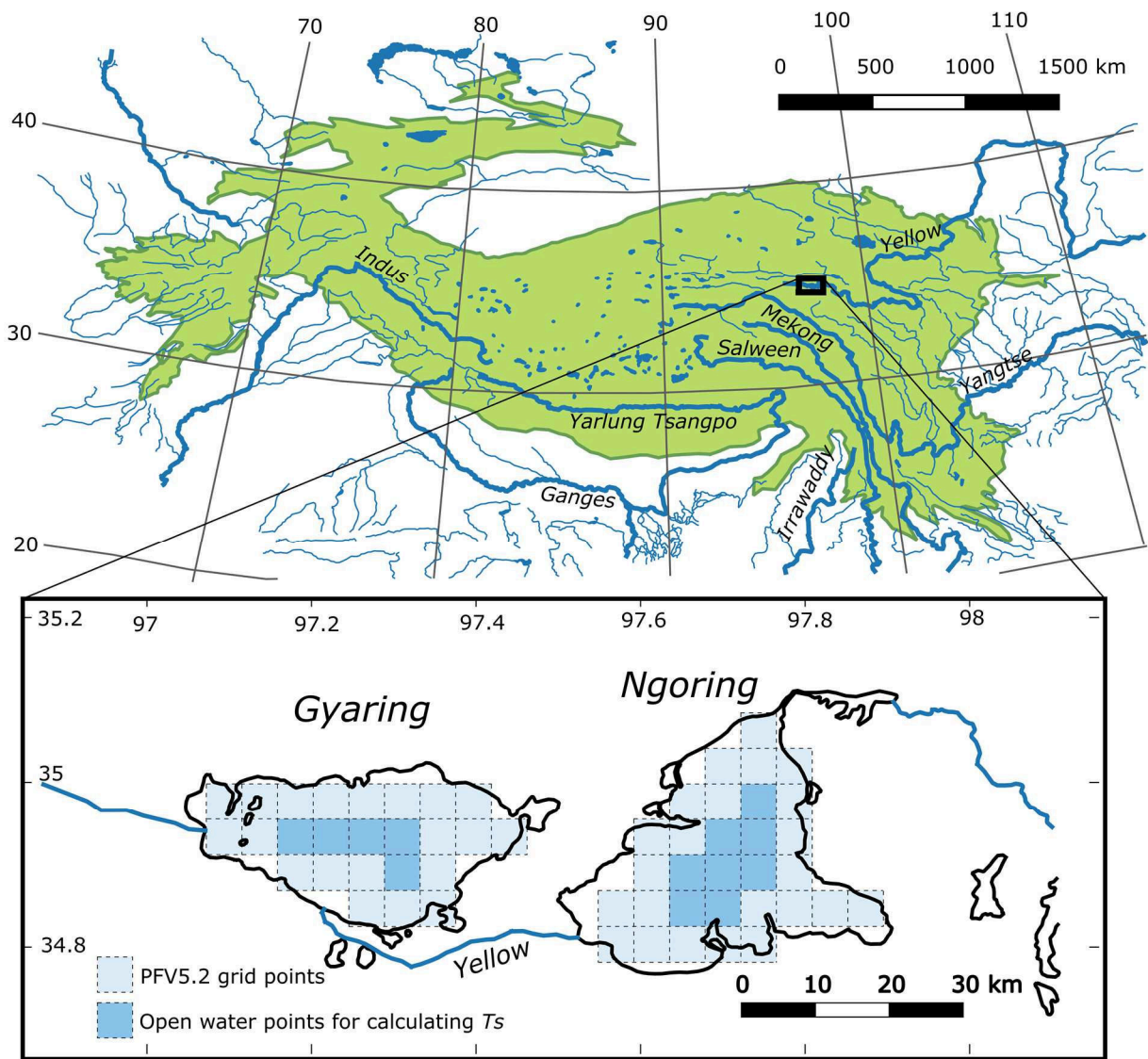
Fig. 1: Study site map and the points of the AVHRR Pathfiner grid used for estimation of the surface temperature from satellite data. The green shaded region is the Tibetan Plateau, shown as land above 2000 m a.s.l.
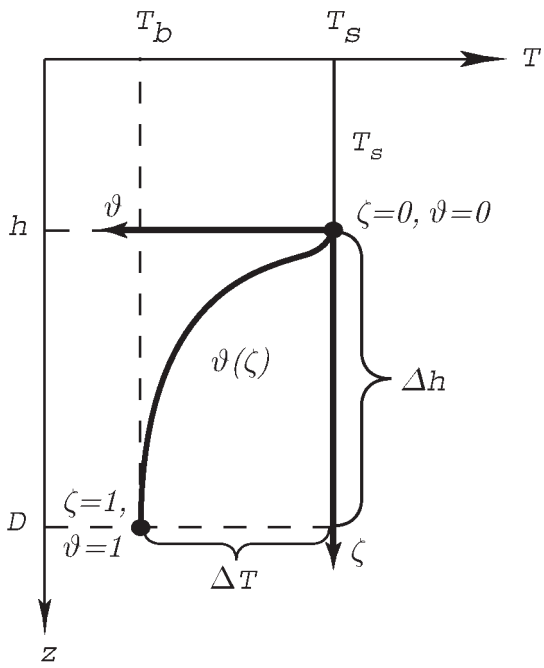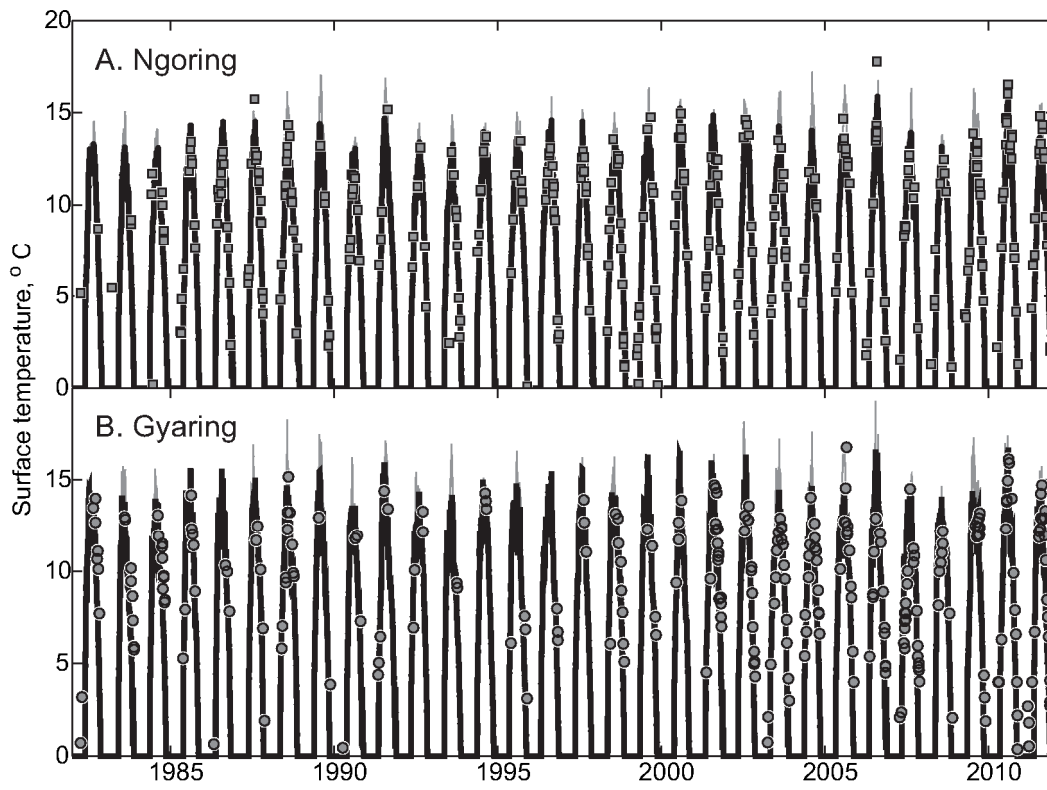
Fig. 2: Schematic of a vertical temperature profile in a thermally stratified lake and the corresponding self-similarity coordinates. See Eqs. (1)-(2) for symbols' meaning.

5

26

Fig. 3: Modeled lake surface temperatures (lines) and the Pathfinder SST data (symbols) for 1982-2012 in (a) Ngoring and (b)
Gyaring. Thick lines are from the Flake model forced by the ERA-Interim reanalysis, thin gray lines are from NCEP/NCAR forcing.
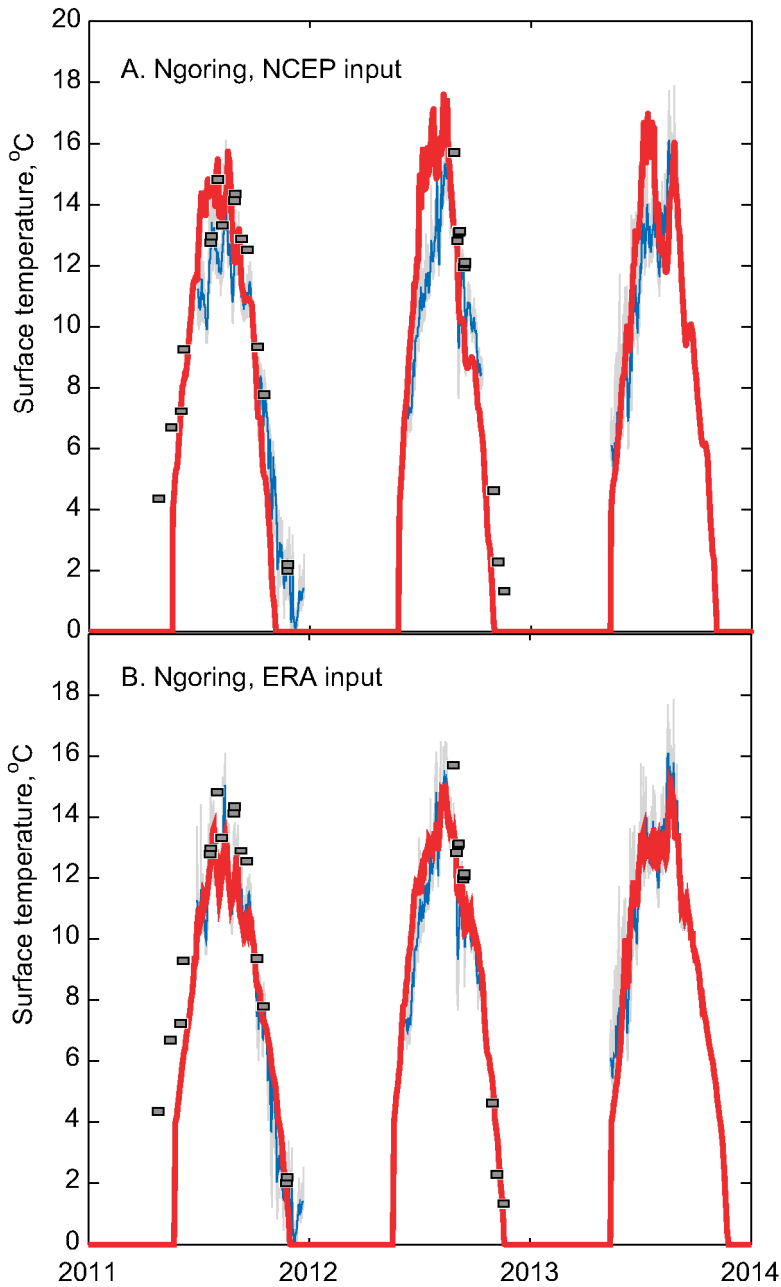
Fig. 4: Comparison of results from the Flake model forced by (a) NCEP/NCAR and (b) ERA-Interim reanalyses against the in-situ lake surface temperatures in Ngoring. Thick solid (red) lines are model predictions; thin solid (blue) lines are in situ bulk temperatures at 0.5 m depth; Half-tone (gray) lines are the skin surface temperatures determined from the upward long-wave radiation (Li et al. 2016); symbols are the available T_s estimations from satellite data.
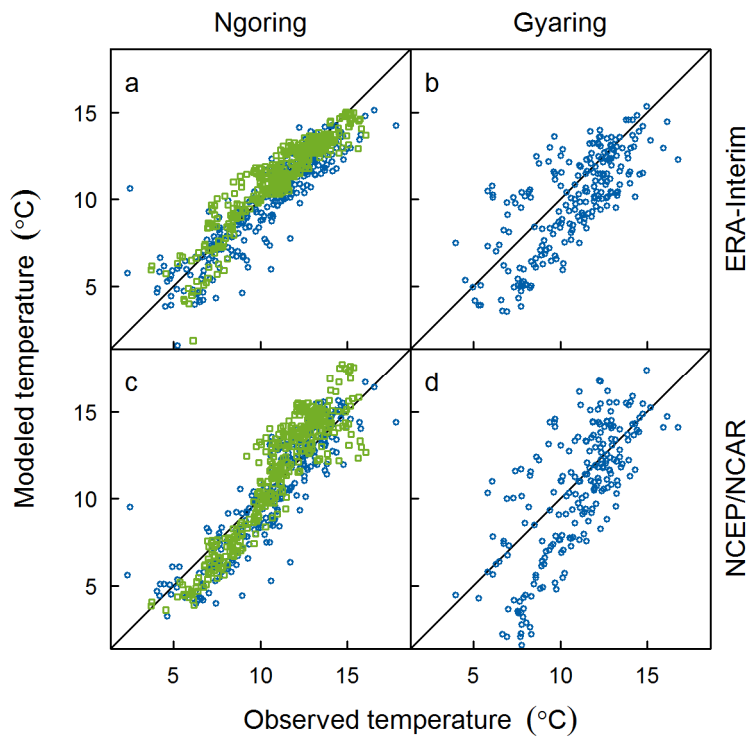
Fig. 5: Comparison of observed and modeled lake surface temperatures in Ngoring (a, c) and Gyaring (b, d) forced by the ERA-Interim reanalysis (a, b) and the NCEP/NCAR reanalysis (c, d). Blue circles are derived from satellite data and green squares from in-situ measurements. Only values from May to October are shown.
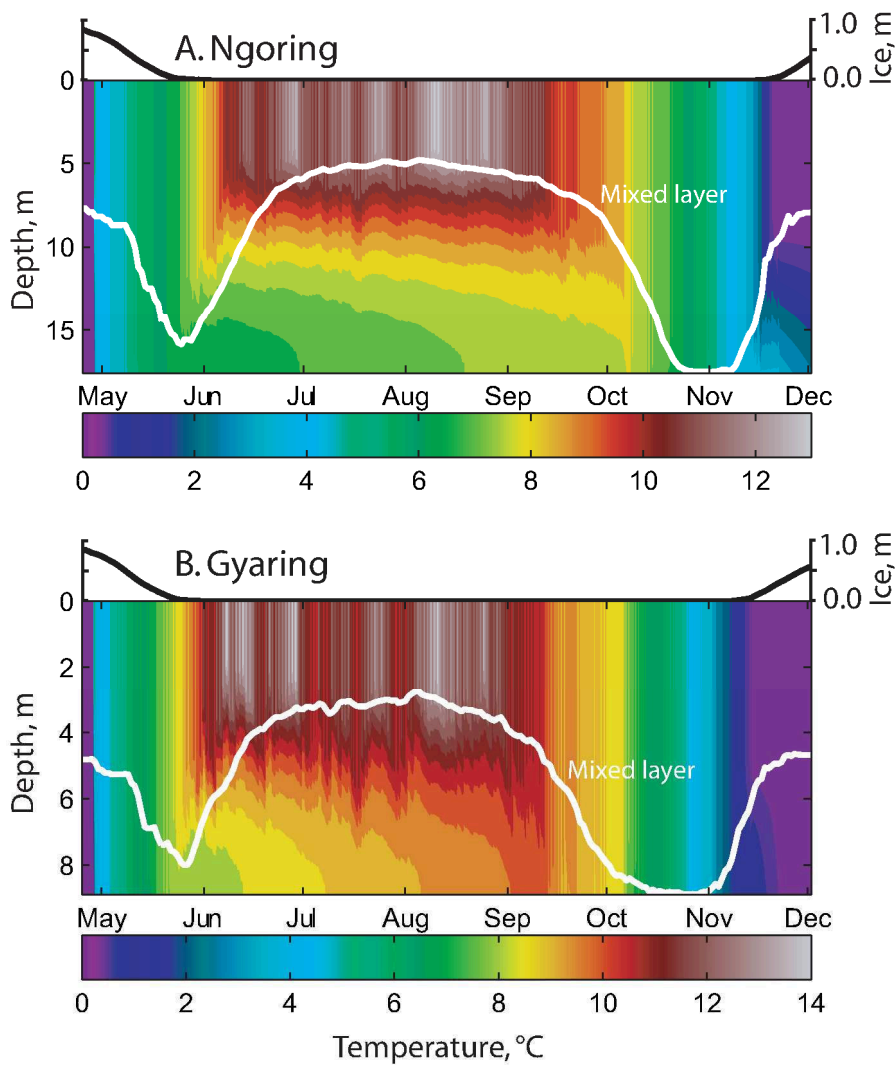
5

29

Fig. 6: Modeled seasonal thermal stratification pattern and ice cover development in (a) Ngoring and (b) Gyaring. The model was forced by the ERA-Interim reanalysis. Only values from May to December 1979 are shown. The black line is the ice cover thickness. The white line is the bottom of the surface mixed layer defined as the depth of the maximum vertical temperature gradient.
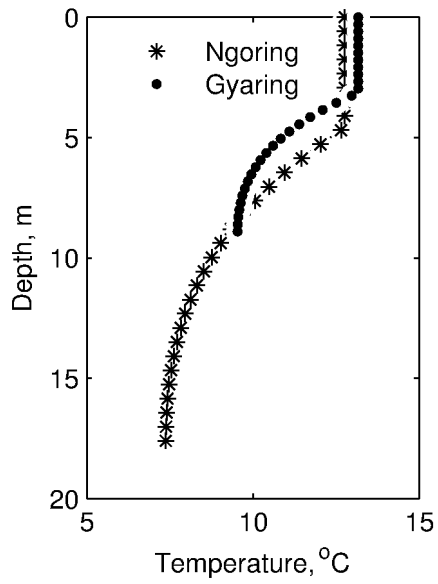
5

30

Fig. 7: Typical modelled vertical profiles of temperature in Ngoring (stars) and Gyaring (circles) in the middle of the summer stratification period (12 Aug 1979).
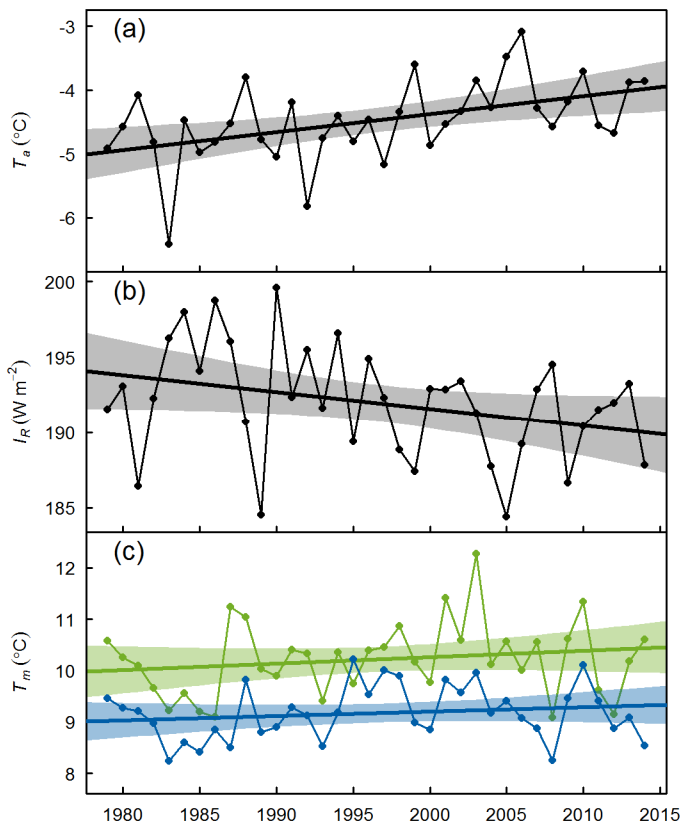
Fig. 8: Trends in annual mean air temperature (a) and solar radiation (b) from ERA-Interim, as well as trends in modeled mean summer lake temperature (c) in Ngoring (blue) and Gyaring (green).